Widths of LWR and LWP Trailed Spectra

C.A. Grady and M.P. Garhart
April 7, 1988

1. Introduction

Oliversen (1986b) noted that the ratio of point source to trailed spectra obtained as part of the on-going recalibration of the IUE cameras showed a larger spread than expected. In order to determine whether the variation in the trailed spectra is due to camera repeatability, problems with the trail procedure at high trail rates, or observing conditions at the time of the observations, we have analyzed trailed spectra for 10 stars included in Oliversen's analysis for the LWR and 7 stars for the LWP.

2. Data Selection Criteria

LWR: The trailed LWR spectra chosen for this study were those analyzed by Oliversen (1986b). The majority of the spectra were processed prior to 1985 October 1 with 55 lines perpendicular to the dispersion direction (Turnrose and Thompson 1984). All of the LWR spectra were processed using ITF2, the newest ITF for that camera which has not yet been used for routine processing of spectral data. Five of the LWR spectra (3 of η UMa, 1 of ζ Cas, and 1 of 10 Lac) were processed after 1985 October 1 as extended line-by-line files with 110 lines perpendicular to the dispersion direction (Munoz Preiro 1985). A total of 33 spectra are involved, and are tabulated in Table 1.

LWP: The LWP spectra included in our analysis were observed from late 1985 through mid 1986. This time interval was chosen to ensure that any high trail rate observations were made using the fast trail technique (Oliversen 1986a), resulting in uniform illumination of the large science aperture. We have excluded more recent observations to minimize the effects of camera sensitivity changes as a function of time (Sonneborn and Garhart, 1987). We have also excluded any calibration stars with fewer than two trailed spectra in the study interval. The IUE calibration star observations were supplemented by fast trailed spectra of Vega (HD 172167), in order to have additional data at high trail rates. A total of 42 spectra, all but 5 of which were obtained using the 2 gyro control mode are included. All of the spectra were processed with LWP ITF 1, the ITF in routine use for data processing for data processed prior to 1987 December. The majority of the LWP spectra were processed after 1985 October 1 and have the extended line-by-line format with 110 lines perpendicular to the dispersion direction. The journal of observations is given in Table 2.

3. Analysis Technique

Our analysis has been restricted to the spatially resolved spectral data files. The net integrated FN in four 100 Å wide bandpasses, centered at 1900, 2300, 2700, and 3100 Å,were estimated from

$$Net = \sum_{a \leq l \leq b} \sum_{w_1 \leq w \leq w_2} (F_{lw} - B_{lw}) \quad (1)$$

where F_{lw} are the flux numbers in the line-by-line or extended line-by-line spectral files, and w_1 and w_2 are the wavelength limits for the summation in each bandpass. The background, B_{lw}, at the position of the spectrum was estimated by first masking out the portion of the line-by-line or extended line-by-line data involving the spectrum, and then fitting the remaining data to a straight line. The summation over the line numbers runs from $a = 34$ to $b = 74$ for the extended line by line format spectra, and from lines $a = 17$ to $b = 34$ for the data processed prior to 1 October 1985.

The average peak flux in the spectrum at each bandpass was calculated from

$$AveragePeakFlux = \left(\frac{1}{n} \sum_{c \leq l \leq d} \sum_{w_1 \leq w \leq w_2} F_{lw} - B_{lw} \right) \tag{2}$$

In order to compensate for the difference in the processing of the extended line by line and older data, 15 lines (n) are summed over for the extended line-by-line format, and 8 for the line-by-line format. The starting and stopping lines for the integration are lines 25 and 32 respectively for the line-by-line data and 50 and 64 for the extended line-by-line.

The effective width of the spectrum in each bandpass is

$$Width = Net \Big/ AveragePeakFlux \tag{3}$$

4. Results

LWR: The effective spectral widths for the LWR data are presented in Table 1. Figure 1 shows the spectral widths as a function of trail rate at 2300 Å. Figure 2 shows the data plotted as a function of radiation background, and Figure 3 as a function of THDA. The spectrum with the smallest spectral width, LWR 17583, was obtained with a radiation background FPM=2.7 V, and was also obtained with the hottest camera, THDA=17.2. There is a suggestion that the spectral width may be weakly anti-correlated with THDA, since the spectra with the largest widths tend to be those obtained with the lowest THDA. Sonneborn and Garhart (1987) note that the camera sensitivities are anti-correlated with THDA, and that this effect is largest for the LWR. The LWR data considered in this study cover a range of THDA corresponding to a 5 percent decrease in sensitivity, and most of the scatter about a mean effective spectral width is close to this value. These results suggest that the trail rate by itself is not the most important factor in determining the effective spectral width, although the available spectra are too few to be conclusive.

LWP: The LWP dataset includes proportionally many more spectra obtained at high trail rates and with a wider range of radiation backgrounds and THDA values than the LWR dataset. Figure 4 shows the spectral widths as a function of trail rate for all four bandpasses. The scatter in the spectral width is similar for both the low and high trail rate spectra. This suggests that if the observation has been made using the fast trail technique, the trailing procedure is not systematically underilluminating the aperture for the observations made with higher trail rates. Figure 5 shows the same data plotted as a function of the radiation level. The three spectra from Figure 4 which had comparatively small spectral widths are spectra which were obtained during high radiation backgrounds. These data suggest that for radiation backgrounds below FPM=1.5, there is little effect on the spectral width, but that high radiation background images have systematically narrower spectral widths. Figure 5 shows the width data plotted as a function of the background DN level, as recorded on the scripts. Figure 6 shows the radiation-induced background per hour for the spectra included in this study.

4. Interpretation

Oliversen (1984b) evaluated linearity errors in LWR spectra processed with the same ITF as was used to process the LWR spectra included in this study. Images obtained with a high radiation background were found to have overestimated the flux amplitude by five to 10 percent from 2400 to 3000 Å. This sort of overestimation would result in an overestimate of the average peak flux, and hence result in depressed effective spectral widths. This may account for the small effective trail widths in LWR 17583 and LWR 17588. Since other high FPM spectra do not show the depressed spectral widths in the LWR other factors, independent of both trail rate and FPM, may be present. The slight elevation of the η UMa effective spectral widths may also reflect the fact that fast trail procedure is not completely reproducible, with a fraction of otherwise operationally identical observations (back up distance, wheel speeds, back up rate, β angle, etc.), resulting in the star grazing the large aperture, or in the case of the data considered here, slightly non-uniformly illuminating the aperture.

Oliversen (1984a) in an analysis of LWP spectra processed with the ITF used to reduce these data found that high radiation background spectra also systematically overestimated the slit integrated flux compared to optimally exposed and low background images. The magnitude of the overestimate was a strong function of wavelength. For this camera, the three spectra with particularly small effective spectral widths were all obtained with high radiation backgrounds, implying that linearity errors are responsible for much of the scatter in point source to trailed spectral ratios for this camera. Since the correlation with radiation is not present for data obtained with FPM$\leq$1.5, we suggest that any high radiation background data be excluded from the absolute calibration. These results may not be applicable to LWP spectra processed with the most recent ITF, in routine use since 1987 December.

References

Munoz Preiro, J.R. 1985, IUE NASA Newsletter, 27, 27.

Oliversen, N.A. 1984a, IUE NASA Newsletter 24, 27.

Oliversen, N.A. 1984b, IUE NASA Newsletter 24, 57.

Oliversen, N.A. 1986a, IUE NASA Newsletter 31, 40.

Oliversen, N.A. 1986b, "LWR Absolute Calibration Progress Report, October 20 1986", Report to the 3-Agency Meeting, November 1986.

Sonneborn, G., and Garhart, M.P. 1987, IUE NASA Newsletter, 33, 78.

Turnrose, B.E., and Thompson, R.W. 1984, IUE Spectral Image Processing System, Version 2.2 (New Software), CSC/TM-84/6058.

Table 1: Journal of LWR Observations

Image	Trail Rate	FPM	THDA	ELBL	Spectral Widths (lines)			
					1900	2300	2700	3100
ζ Cas								
17438	16.67	2.37	14.5	No	10.49	10.48	10.28	9.45
17786	17.39	1.0	15.5	Yes	10.75	10.37	10.65	9.89
η Aur								
17594	20.83	1.8	16.2	No	10.10	10.62	10.44	10.00
17652	20.83	0.7	13.2	No	10.77	10.73	10.46	10.36
λ Lep								
17557	15.38	1.05	14.8	No	11.42	11.01	10.65	11.74
17558	15.38	1.7	14.8	No	10.48	10.78	10.48	9.85
μ Col								
17548	8.26	0.08	16.2	No	10.92	10.93	10.57	10.94
17550	8.26	0.7	16.2	No	10.76	10.77	10.41	10.22
17656	8.00	0.88	15.5	No	10.73	10.69	10.37	10.13
17657	8.00	1.19	15.9	No	10.78	10.80	10.50	10.07
η UMa								
17745	69.0	0.08	13.2	Yes	11.65	11.55	10.89	12.17
17823	69.0	1.11	11.2	Yes	10.78	10.64	10.63	10.06
17824	69.0	0.39	11.5	Yes	11.15	11.00	10.87	10.27
10 Lac								
17582	8.26	2.4	16.9	No	10.50	10.54	10.36	9.88
17583	8.26	2.7	17.2	No	7.45	8.74	9.38	6.33
17719	8.26	1.40	14.2	Yes	10.64	10.83	10.43	10.17
HD 60753								
17462	0.64	1.94	15.2	No	10.27	10.60	10.39	9.79
17609	0.64	2.0	15.9	No	10.54	10.83	10.46	10.32
17662	0.64	0.08	12.5	No	10.63	10.54	10.45	10.06
17666	0.64	0.08	14.2	No	10.22	10.47	10.40	9.94
17670	0.64	0.12	14.2	No	10.71	10.74	10.43	10.03
17687	0.64	0.08	14.5	No	9.99	10.70	10.46	10.30
17658	0.64	1.79	15.9	No	10.27	10.60	10.37	9.85
17688	0.64	0.08	14.8	No	10.59	10.73	10.50	10.27
BD+75 325								
17571	0.19	0.68	16.2	No	10.49	10.78	10.38	9.94
17622	0.19	0.08	16.5	No	10.43	10.46	10.27	9.84

Table 1: Journal of LWR Observations (*cont.*)

Image	Trail Rate	FPM	THDA	ELBL	Spectral Widths (lines)			
					1900	2300	2700	3100
HD 93521								
17693	1.43	0.08	15.2	No	10.99	10.98	10.61	10.79
17694	1.43	0.08	15.2	No	10.71	10.78	10.44	10.41
17618	1.43	0.08	16.2	No	10.85	10.83	10.47	10.32
17617	1.43	0.08	16.2	No	10.61	10.66	10.28	10.22
BD+28 4211								
17713	0.25	1.16	14.2	No	9.53	10.06	10.00	8.74
17712	0.25	0.73	13.8	No	10.15	10.40	10.17	9.3
17588	0.26	1.9	13.8	No	8.73	9.44	9.54	6.47

Table 2: LWP Journal of Observations

Image	Trail Rate	FPM	THDA	ELBL	Spectral Widths (lines)			
					1900	2300	2700	3100
ζ Cas								
6692	20.8	0.08	7.5	No	11.0	10.6	11.1	11.8
9134	20.8	0.08	7.2	Yes	10.3	10.4	10.3	12.2
9140	20.8	0.08	7.5	Yes	11.0	10.2	10.2	12.3
BD+75 325								
5703	0.20	0.35	10.2	No	10.8	11.0	11.3	13.4
6731	0.20	0.08	9.2	No	10.7	11.0	11.3	12.6
7601	0.20	0.3	10.8	Yes	10.9	10.3	10.3	12.7
HD 93521								
6004	1.80	0.08	7.8	No	13.1	11.0	11.5	14.0
9602	1.80	0.13	10.2	Yes	11.1	10.5	10.5	14.6

Table 2: Journal of Observations (*continued*)

Image	Trail Rate	FPM	THDA	ELBL	Spectral Widths (lines)			
					1900	2300	2700	3100
η UMa								
7208	88.5	2.52	11.2	Yes	7.2	8.3	9.1	6.0
7209	88.5	2.02	11.5	Yes	9.8	9.9	10.1	9.8
7218	88.5	2.44	9.5	Yes	7.0	8.6	9.3	7.0
8376	88.5	1.5	10.2	Yes	10.5	10.2	10.2	10.8
8377	88.5	1.2	10.2	Yes	10.8	10.3	10.2	11.2
8378	88.5	0.50	10.2	Yes	11.5	10.4	10.3	12.1
HD 60753								
5576	0.78	0.4	9.8	No	11.1	10.7	11.2	12.5
6352	0.78	1.61	9.5	No	10.1	10.3	11.1	10.9
6799	0.78	0.08	9.8	No	10.8	10.5	11.1	12.1
6804	0.78	0.6	11.2	No	10.8	10.6	11.2	11.8
6806	0.78	0.95	11.2	No	10.7	10.6	11.2	11.9
7629	0.78	1.36	9.5	Yes	11.1	10.4	10.3	11.8
8050	0.78	0.08	6.1	Yes	11.0	10.2	10.3	11.8
8054	0.78	0.08	7.2	Yes	11.4	10.3	10.3	12.0
8059	0.78	0.08	7.5	Yes	11.5	10.3	10.4	12.1
8138	0.78	0.13	9.8	Yes	11.4	10.7	10.6	12.2
8506	0.78	1.35	10.8	Yes	11.4	10.3	10.3	11.9
8508	0.78	0.08	11.2	Yes	11.6	10.6	10.4	12.5
8756	0.78	0.08	9.2	Yes	11.9	10.6	10.4	12.3
8800	0.78	2.63	8.5	Yes	6.4	7.9	9.1	6.0
8802	0.78	1.66	8.8	Yes	10.8	10.1	10.2	10.8
9263	0.78	0.08	8.8	Yes	11.6	10.4	10.4	12.5
9267	0.78	0.34	9.5	Yes	11.0	10.3	10.3	12.0
BD+28 4211								
6040	0.10	0.15	8.8	No	10.5	10.7	11.1	12.4
6104	0.10	0.08	9.5	No	11.0	10.8	11.3	14.1
6674	0.10	0.08	9.8	No	10.7	10.7	11.2	12.8
8991	0.10	0.08	6.8	Yes	10.8	10.3	10.4	12.7
8992	0.10	0.08	6.8	Yes	11.0	10.3	10.4	12.4
9372	0.10	0.08	9.5	Yes	10.9	10.2	10.2	12.2
9373	0.10	0.08	9.5	Yes	10.5	10.1	10.2	11.9
9729	0.10	0.08	10.8	Yes	10.6	10.7	10.8	14.0
α Lyr								
7010	95.0	0.08	10.2	Yes	10.4	10.4	10.4	11.7
7888	100.00	0.08	8.5	Yes	11.6	10.3	10.3	11.4
7889	100.00	0.36	8.8	Yes	11.5	10.4	10.3	11.6

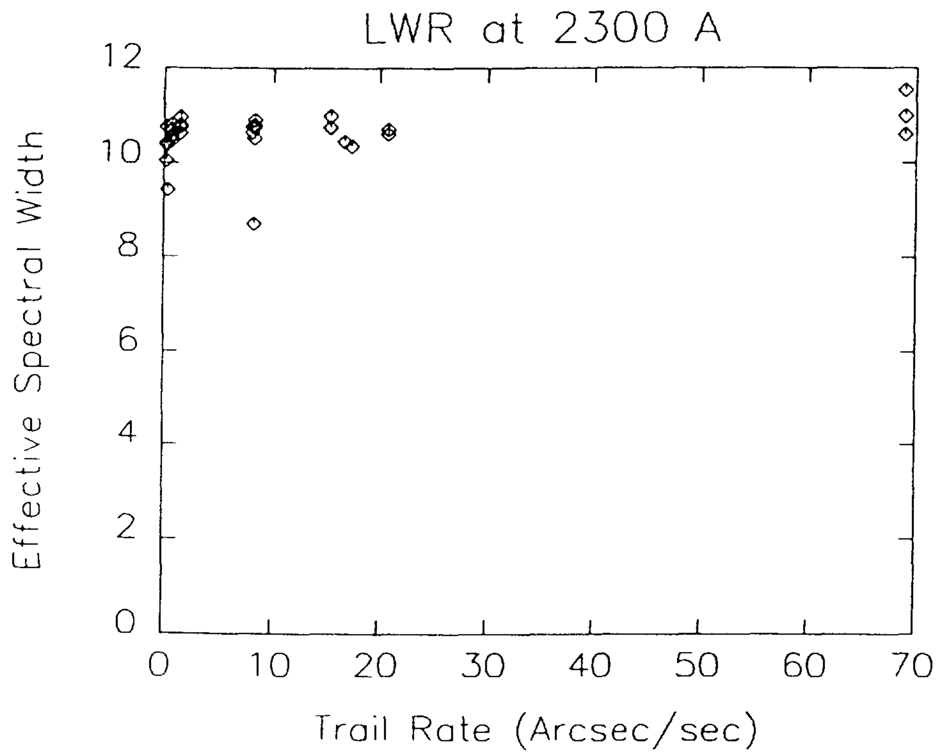

Figure 1: LWR trailed spectral widths in the 2300 Å bandpass as a function of trail rate.

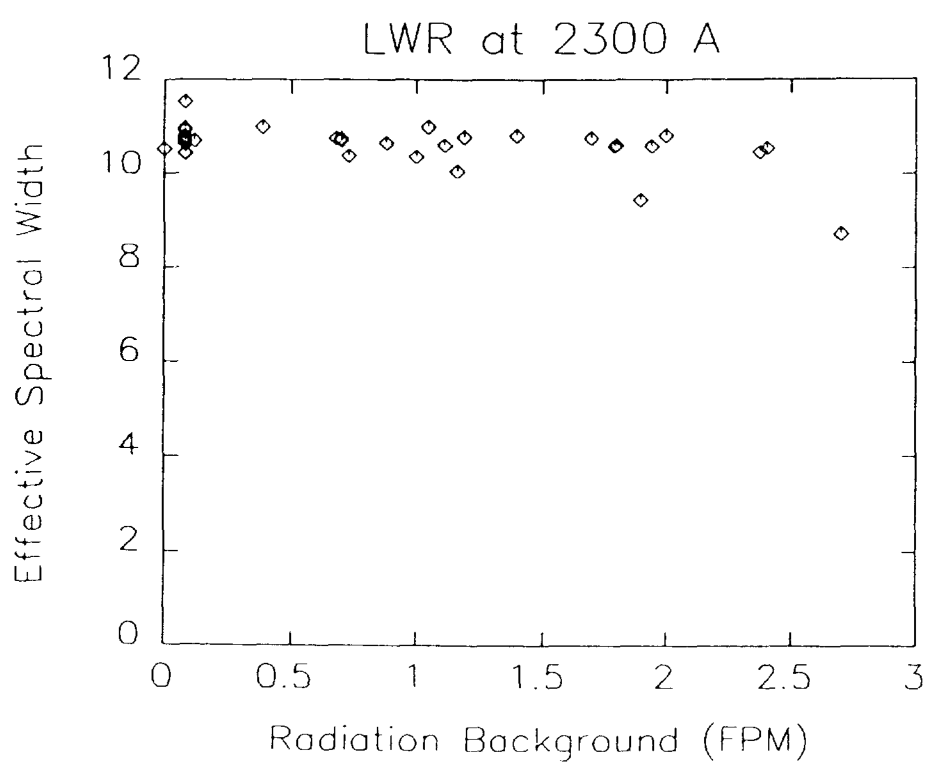

Figure 2: LWR trailed spectral widths as a function of radiation background (FPM).

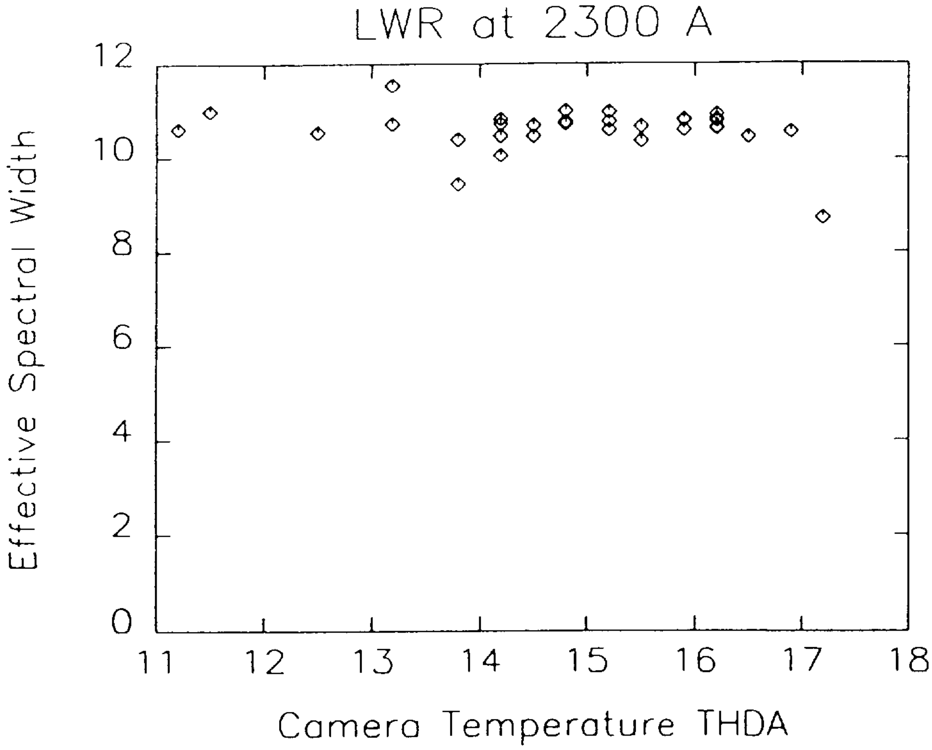

Figure 3: LWR trailed spectral widths as a function of THDA.

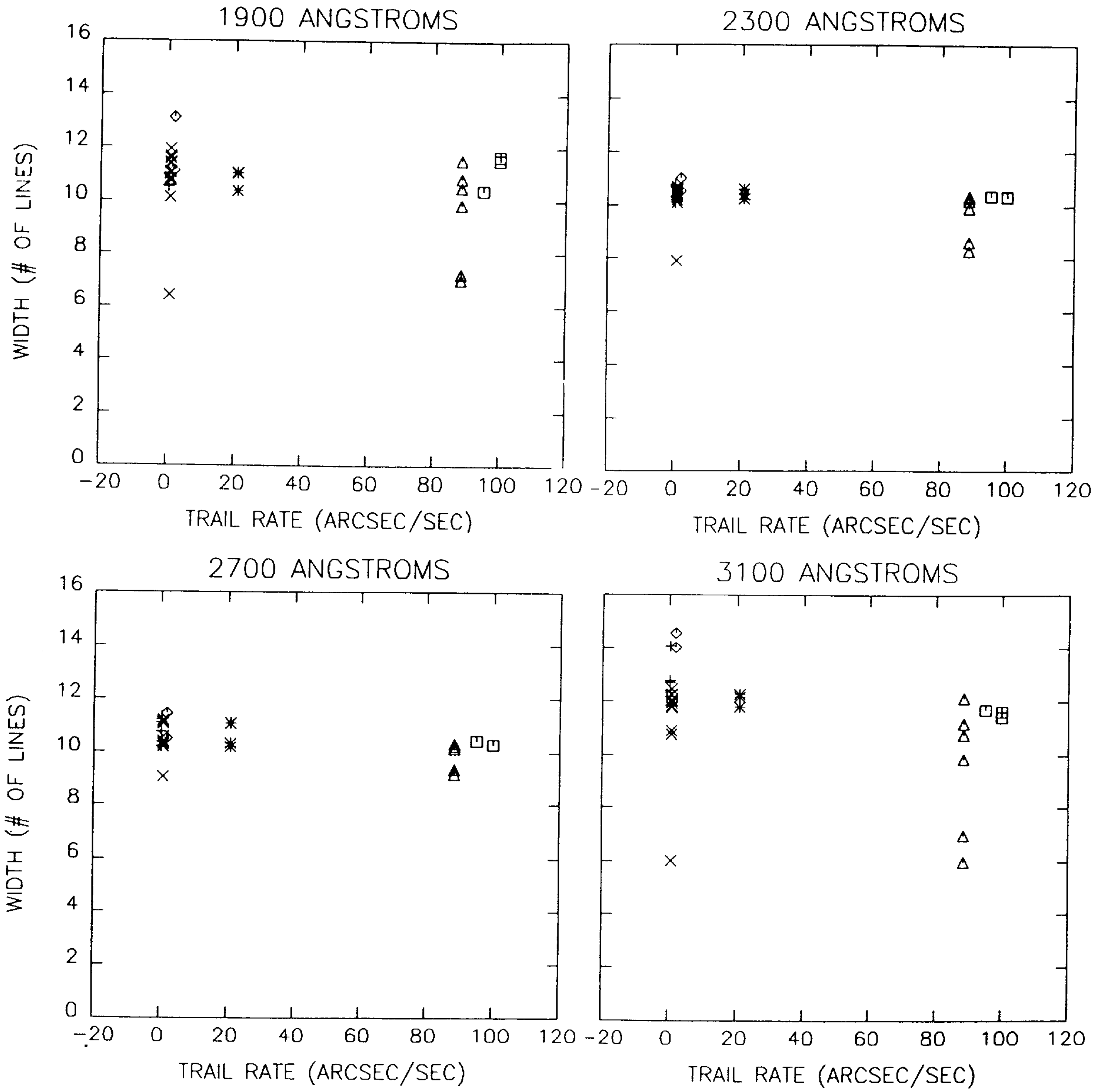

Figure 4: LWP trailed spectral widths as a function of trail rate.

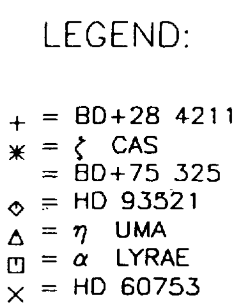

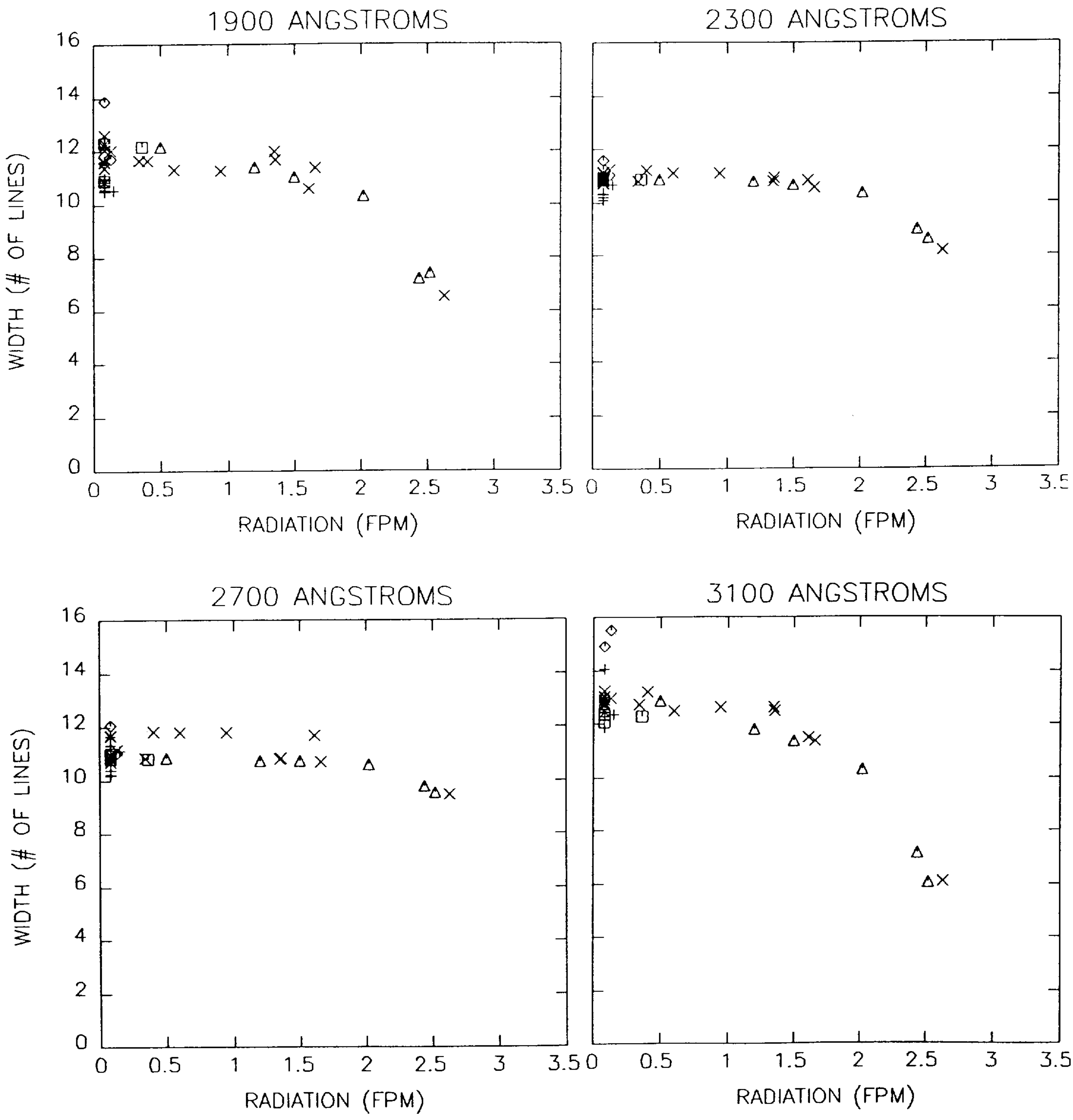

Figure 5: LWP trailed spectral widths as a function of radiation background.

LEGEND:

+ = BD+28 4211
✳ = ζ CAS
= BD+75 325
◇ = HD 93521
△ = η UMA
□ = α LYRAE
× = HD 60753

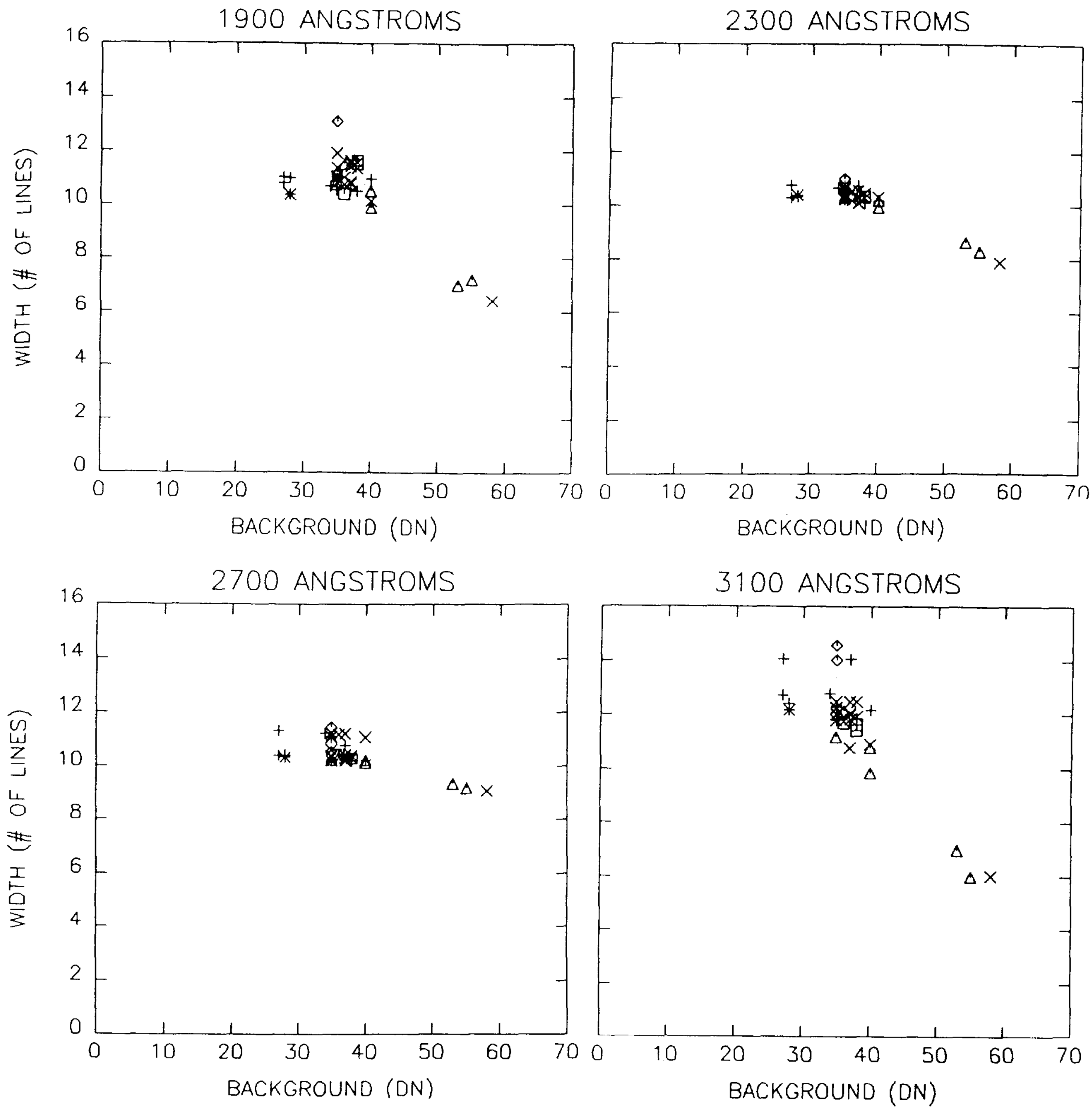

Figure 6: LWP trailed spectral widths as a function of background DN.